Victor Iliev Rizov[1*], *Holm Altenbach*[2]

LENGTHWISE FRACTURE OF INHOMOGENEOUS VISCOELASTIC BEAM THAT MOVES AT A VARYING ACCELERATION: A STUDY CONSIDERING ENERGY DISSIPATION

PODUŽNI LOM NEHOMOGENOG VISKOELASTIČNOG NOSAČA KOJI SE POMERA PROMENLJIVIM UBRZANJEM: STUDIJA SA RAZMATRANJEM DISIPACIJE ENERGIJE

Originalni naučni rad / Original scientific paper
Rad primljen / Paper received: 15.04.2025
https://doi.org/10.69644/ivk-2026-01-0158

Adresa autora / Author's address:
[1)] University of Architecture, Civil Engineering and Geodesy, Department of Technical Mechanics, 1 Chr. Smirnesky blvd., 1046 - Sofia, Bulgaria [*]email: v_rizov_fhe@uacg.bg

V.I. Rizov https://orcid.org/0000-0002-0259-3984
[2)] Lehrstuhl für Technische Mechanik und Geschäftsführender, Institut für Mechanik G10/58, Fakultät für Maschinenbau, Otto-von-Guericke-Universität Magdeburg, Universitätsplatz 2, 39106 Magdeburg, Deutschland
H. Altenbach https://orcid.org/0000-0003-3502-9324

Keywords
- continuously inhomogeneous beam
- lengthwise fracture
- varying acceleration
- energy dissipation

Ključne reči
- kontinualno nehomogeni nosač
- podužni lom
- promenljivo ubrzanje
- disipacija energije

Abstract

The application of continuously inhomogeneous structural materials in various spheres of modern engineering constantly increases. Very often these materials are used for manufacturing different members and components of machines and mechanisms which perform non-uniform motion. Inertia loads generated by acceleration have to be taken into account when studying fracture in non-uniformly moving members. The current paper concentrates on the effect of energy dissipation on lengthwise fracture in a continuously inhomogeneous beam member that moves up at a varying acceleration. The beam has nonlinear viscoelastic behaviour. A theoretical model with a linear spring and a nonlinear dashpot subjected to time-dependent stress is applied for describing the viscoelastic behaviour of the beam. There are two symmetric lengthwise cracks in the moving beam. The lengthwise fracture under the action of the inertia loads is analysed by the J integral. The effect of energy dissipation is taken into account in the analysis by using the reduced specific strain energy. The latter is extracted from the stress in the spring only (the dashpot dissipates the energy). The J integral solution is checked-up by deriving the strain energy release rate in the beam under inertia loads with considering the effect of energy dissipation. A detailed analysis of the influence of the acceleration of the beam, energy dissipation, mass distribution, and parameters of the viscoelastic model on lengthwise fracture is performed. Applications of the analysis in structural design of moving beams with taking into account the energy dissipation are presented.

Izvod

Primene kontinualno nehomogenih konstrukcionih materijala u raznim sferama modernog inženjerstva su u stalnom porastu. Često se ovi materijali koriste za izradu raznih elemenata i komponenata mašina i mehanizama koji se kreću neuniformno. Inercijalna opterećenja koja nastaju ubrzanjem treba da se uzimaju u obzir u istraživanju loma kod neuniformnog kretanja delova. U ovom radu se fokusiramo na uticaj disipacije energije na podužni lom kontinualno nehomogenog elementa nosača, koji se pomera nagore promenljivim ubrzanjem. Nosač se ponaša nelinearno viskoelastično. Za opisivanje viskoelastičnog ponašanja nosača primenjuje se teorijski model sa linearnom oprugom i prigušivačem, a koji je opterećen vremenski zavisnim opterećenjem. U pokretnom nosaču postoje dve simetrične podužne prsline. Za analizu podužnog loma pod dejstvom inercijalnih opterećenja koristi se J integral. U analizi se uticaj disipacije energije uzima u obzir korišćenjem redukovane specifične energije deformacije, koja se dobija iz napona, samo u opruzi (energija u prigušivaču se gubi). Rešenje J integrala se proverava izvođenjem brzine oslobađanja energije deformacije nosača pod inercijalnim opterećenjem, uz razmatranje uticaja energije disipacije. Data je detaljna analiza uticaja: ubrzanja nosača, energije disipacije, raspodele mase, i parametara viskoelastičnog modela, na podužni lom. Prikazana je primena analize u projektovanju konstrukcija pokretnih nosača sa razmatranjem disipacije energije.

INTRODUCTION

The advance in various spheres of engineering depends in a high extent on utilisation of modern structural materials. Therefore, developing and introducing of new materials is a constant task for the international engineering community. Continuously inhomogeneous (functionally graded) materials are a typical example for highly efficient new composites which attract the attention of engineers and researchers /1-3/. Due to their unique properties, the continuously inhomogeneous materials are growingly used especially in high-tech areas like aeronautics, microelectronics, nuclear reactors and optics /4-6/. One of the most important advantages of these materials is the fact that their properties vary continuously in a solid. Besides, the variation of properties can be designed for achieving of some predefined goals which opens a wide application of prospects /7-9/. Studying of fracture in structural members made by continuously inho-

mogeneous materials contributes significantly for guaranteeing safety and reliability of structures and facilities /10-12/. Although research in the field of fracture mechanics of continuously inhomogeneous materials and structures has progressed in the recent decades, there are some problems that need more attention. For instance, application of these materials for manufacturing of various members and components of different machines and mechanisms constantly grows. These members and components very often are designed to perform non-uniform motion. The acceleration experienced by non-uniformly moving members and components induces inertia loads that have to be considered when analysing fracture behaviour. Besides, a particular issue when dealing with fracture in structural components having viscoelastic behaviour is the energy dissipation and its effect on the fracture performance.

The current paper is concentrated on analysing the effect of energy dissipation on the lengthwise fracture in a continuously inhomogeneous nonlinear viscoelastic beam that moves up at a varying acceleration. The viscoelastic behaviour of the beam is treated by a model with a nonlinear elastic spring and a linear dashpot under a varying stress. The lengthwise fracture in the beam under varying inertia load is analysed by the J integral. In order to take into account the effect of the energy dissipation, the specific strain energy that is used when solving the J integral is obtained only from the stress in the spring of the viscoelastic model because the dashpot dissipates energy. A check-up of the solution of the J integral is carried-out by deriving the SERR (strain energy release rate) in the beam under inertia load with taking into account the energy dissipation (for this purpose, the specific complementary strain energy involved in the SERR solution is found by analysing only the stress in the spring of the viscoelastic model). The results of analysis of the influence of various parameters (acceleration, energy dissipation, distribution of the properties of the viscoelastic model and the mass across the beam thickness) on the lengthwise fracture are presented. It is shown also that the current fracture analysis can be applied in structural design of non-uniformly moving continuously inhomogeneous nonlinear viscoelastic beams with taking into account the energy dissipation by using the principles of fracture mechanics.

THEORETICAL MODEL AND ANALYSIS

Consider the rectangular beam member shown in Fig. 1.

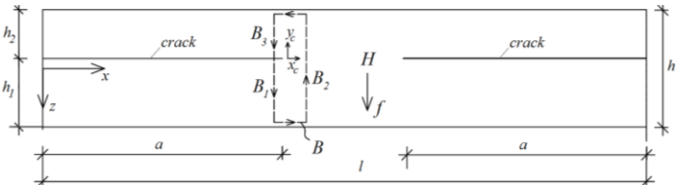

Figure 1. Scheme of the beam with lengthwise cracks.

The beam hosts two lengthwise cracks each of length a. The cracks are symmetric with respect to the mid-span. The beam moves up at a varying acceleration a_{uw}. Equation (1) describes the variation of a_{uw} with time t,

$$a_{uw} = n_1 t^s + n_2 t^r , \tag{1}$$

where: n_1, n_2, s, and r are parameters.

The mass per unit area of the beam is marked by m_1. The beam is continuously inhomogeneous across its thickness, h. The variation of m_1 across the beam thickness is described by the law in Eq. (2),

$$m_l = m_{lup} + \frac{m_{llw} - m_{lup}}{h^{\delta_1}} \left(\frac{h}{2} + z \right)^{\delta_1} , \tag{2}$$

$$-\frac{h}{2} \le z \le \frac{h}{2} , \tag{3}$$

where: m_{lup} and m_{llw} are the mass per unit area on the upper and lower surface of the beam; z is the vertical centric axis (Fig. 1); δ_1 is a parameter.

The intensity of the time-dependent inertia load, f_ϕ, in an arbitrary point, H, of the beam is obtained by Eq. (4),

$$f_\varphi = -a_{uw} m_l . \tag{4}$$

It should be noted that f_ϕ is directed downwards since the beam acceleration is directed upwards.

The distributed deadweight of the beam f_g, is defined by using Eq.(5),

$$f_g = m_l g , \tag{5}$$

where: g is the earth acceleration. The distributed time-dependent load f, that acts in an arbitrary point H of the moving beam is derived by Eq.(6),

$$f = f_\varphi + f_g . \tag{6}$$

By using Eqs.(1), (2), (4), (5), and (6), we obtain

$$f = \left[n_1 t^s + n_2 t^r + g \right] \left[m_{lup} + \frac{m_{llw} - m_{lup}}{h^{\delta_1}} \left(\frac{h}{2} + z \right)^{\delta_1} \right] . \tag{7}$$

Equation (7) indicates that f varies continuously across the beam thickness. However, f is constant along the beam length.

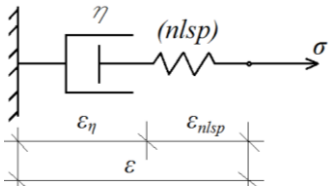

Figure 2. Scheme of the nonlinear viscoelastic model.

The beam has nonlinear viscoelastic behaviour described by the theoretical model shown in Fig. 2. The model consists of a nonlinear spring (*nlsp*), and a linear dashpot with coefficient of viscosity η, as shown in Fig. 2. The model is under stress σ, varying with time according to the law in Eq.(8),

$$\sigma = \alpha + \beta (t^s + t^r) , \tag{8}$$

where: α and β are parameters.

The behaviour of the nonlinear spring is treated by using the stress-strain law in Eq.(9) /13/,

$$\sigma_{nlsp} = \frac{D \varepsilon_{nlsp}}{\sqrt{1 + \varepsilon_{nlsp}}} , \tag{9}$$

where: σ_{nlsp} is stress; ε_{nlsp} is strain; D is a parameter. It is obvious from Fig. 2 that,

$$\sigma_{nlsp} = \sigma . \tag{10}$$

By using Eqs.(8), (9), and (10), we derive

$$\varepsilon_{nlsp} = \frac{1}{2D^2} \left(\sigma^2 + \sigma \sqrt{\sigma^2 + 4D^2} \right) . \tag{11}$$

The behaviour of the linear dashpot in the model in Fig. 2 is treated by using the law in Eq.(12),

$$\sigma_\eta = \eta \dot{\varepsilon}_\eta \,, \quad (12)$$

where: σ_η is stress; $\dot{\varepsilon}_\eta$ is the derivative of strain in the dashpot with respect to time. Apparently (Fig. 2),

$$\sigma_\eta = \sigma \,. \quad (13)$$

By using Eqs.(8), (12), and (13), we derive

$$\varepsilon_\eta = \frac{1}{\eta}\left[\alpha t + \beta\left(\frac{t^{s+1}}{s+1} + \frac{t^{r+1}}{r+1}\right)\right]. \quad (14)$$

The strain ε in the model (Fig. 2) is obtained by Eq.(15),

$$\varepsilon = \varepsilon_\eta + \varepsilon_{nlsp} \,. \quad (15)$$

By using Eqs.(11), (14), and (15), we have

$$\varepsilon = \frac{1}{\eta}\left[\alpha t + \beta\left(\frac{t^{s+1}}{s+1} + \frac{t^{r+1}}{r+1}\right)\right] + \frac{1}{2D^2}\left(\sigma^2 + \sigma\sqrt{\sigma^2 + 4D^2}\right). \quad (16)$$

The stress-strain-time relation in Eq.(16) is used for treating the nonlinear viscoelastic behaviour of the moving beam in Fig. 1 when analysing lengthwise fracture.

Due to material inhomogeneity, the material parameters, D and η, vary across the beam thickness. The laws in Eqs. (17) and (18) describe the variation of D and η, respectively,

$$D = D_{lup} + \frac{D_{llw} - D_{lup}}{h^{\delta_2}}\left(\frac{h}{2} + z\right)^{\delta_2}, \quad (17)$$

$$\eta_l = \eta_{lup} + \frac{\eta_{llw} - \eta_{lup}}{h^{\delta_3}}\left(\frac{h}{2} + z\right)^{\delta_3}, \quad (18)$$

where: D_{up} and D_{lw} are values of D on the upper and lower surface of the beam; η_{up} and η_{lw} are the values of η.

The lengthwise fracture in the beam under inertia loads is analysed by the J integral /14/. Due to the symmetry, only the left-hand half of the beam is considered. In this case, the solution of the J integral is found by Eq.(19),

$$J = 2J_B \,, \quad (19)$$

where: J_B is the value of J integral derived by integrating along contour B around the tip of the left-hand crack (Fig. 1).

Equation (20) expresses J_B, i.e.,

$$J_B = J_{B1} + J_{B2} + J_{B3} \,, \quad (20)$$

where: J_{B1}, J_{B2}, and J_B are values of J in portions, B_1, B_2 and B_3, of the contour, respectively. J_{B1} is presented by Eq.(21),

$$J_{B1} = \int\left[u_{0B1}\cos\alpha_{B1} - \left(p_{xB1}\frac{\partial u_{B1}}{\partial x_c} + p_{yB1}\frac{\partial v_{B1}}{\partial x_c}\right)\right]ds \,, \quad (21)$$

where: u_{0B1} is reduced specific strain energy. Since the dashpot in the viscoelastic model in Fig. 2 dissipates the energy, the reduced specific strain energy is found by integrating the stress in the spring through Eq.(22), i.e.,

$$u_{0B1} = \int \sigma d\varepsilon_{nlsp} \,. \quad (22)$$

The other components of J_{B1} are obtained as given below,

$$\cos\alpha_{B1} = -1 \,, \quad (23)$$

$$p_{xB1} = -\sigma \,, \quad (24)$$

$$\frac{\partial u_{B1}}{\partial x_c} = \varepsilon \,, \quad (25)$$

$$p_{yB1} = 0 \,, \quad (26)$$

$$ds = dz_1 \,, \quad (27)$$

where: σ and ε are the stress and strain in portion B_1 of the integration contour; z_1 is the vertical centric axis of the lower crack arm (it should be noted here that B_1 coincides with the cross-section of the lower crack arm). Apparently,

$$-\frac{h_1}{2} \le z_1 \le \frac{h_1}{2} \,, \quad (28)$$

where: h_1 is lower crack arm thickness.

The stresses and strains in portion B_1 of the integration contour are studied by using Eqs.(29), (30) and (31),

$$\varepsilon = \kappa_1(z_1 - z_{1n}) \,, \quad (29)$$

$$N = \iint\limits_{(A_1)} \sigma dA \,, \quad (30)$$

$$M = \iint\limits_{(A_1)} \sigma z_1 dA \,, \quad (31)$$

where:

$$-\frac{h_1}{2} \le z_1 \le \frac{h_1}{2} \,. \quad (32)$$

Here, κ_1 is curvature, z_{1n} is the neutral axis coordinate, N is axial force, M is bending moment, A_1 is the area of the lower crack arm cross-section. The axial force and bending moment are induced by the distributed law, f. Equations (33) and (34) are applied for obtaining N and M,

$$N = 0 \,, \quad (33)$$

$$M = \frac{a^2}{2}\int\limits_{-h_1/2}^{h_1/2} f dz_1 \,. \quad (34)$$

The MatLab® is used for determining κ_1 and z_{1n} from Eqs.(30) and (31). MatLab is used also for the integration in Eq.(21).

The solution of J_{B2} is found by Eq.(35),

$$J_{B2} = \int\left[u_{0B2}\cos\alpha_{B2} - \left(p_{xB2}\frac{\partial u_{B2}}{\partial x_c} + p_{yB2}\frac{\partial v_{B2}}{\partial x_c}\right)\right]ds \,, \quad (35)$$

where:

$$u_{0B2} = \int \sigma_{B2} d\varepsilon_{nlspB2} \,. \quad (36)$$

$$\cos\alpha_{B2} = 1 \,, \quad (37)$$

$$p_{xB2} = \sigma_{B2} \,, \quad (38)$$

$$\frac{\partial u_{B2}}{\partial x_c} = \varepsilon_{B2} \,, \quad (39)$$

$$p_{yB2} = 0 \,, \quad (40)$$

$$ds = -dz_2 \,. \quad (41)$$

In Eqs.(36)-(41), σ_{B2} and ε_{B2} are the stress and strain in portion B_2 of the integration contour (this portion coincides with beam cross-section ahead of the crack tip), ε_{nlspB2} is the strain in the spring, z_2 is the vertical centric axis of the beam ahead of the crack tip. It is obvious that

$$-\frac{h}{2} \le z_2 \le \frac{h}{2} \,. \quad (42)$$

Equations (43)-(45) are applied for analysing the stresses and strains in portion B_2 of the integration contour,

$$\varepsilon_{B2} = \kappa_2(z_2 - z_{2n}) \,, \quad (43)$$

$$N_{B2} = \iint\limits_{(A_2)} \sigma_{B2} dA \,, \quad (44)$$

$$M_{B2} = \iint\limits_{(A_2)} \sigma_{B2} z_2 dA \,. \quad (45)$$

where:

$$-\frac{h}{2} \le z_2 \le \frac{h}{2} \,. \quad (46)$$

In Eq.(43), κ_2 is curvature, z_{2n} is the neutral axis coordinate. In Eqs.(44) and (45), A_2 is the area of beam cross-section. The axial force and bending moment, N and M, are found by Eqs.(47) and (48),

$$N_{B2} = 0, \tag{47}$$

$$M_{B2} = \frac{a^2}{2} \int_{-h/2}^{h/2} f dz_2 . \tag{48}$$

Equations (44) and (45) are solved for κ_1 and z_{1n} by the MatLab. The integration in Eq.(35) is also performed by MatLab.

Equation (49) is applied for obtaining the solution of J_{B3},

$$J_{B3} = \int \left[u_{0B3} \cos\alpha_{B3} - \left(p_{xB3} \frac{\partial u_{B3}}{\partial x_c} + p_{yB3} \frac{\partial v_{B3}}{\partial x_c} \right) \right] ds . \tag{49}$$

Here,

$$u_{0B3} = \int \sigma_{B3} d\varepsilon_{nlspB3} , \tag{50}$$

$$\cos\alpha_{B3} = -1 , \tag{51}$$

$$p_{xB3} = -\sigma_{B3} , \tag{52}$$

$$\frac{\partial u_{B3}}{\partial x_c} = \varepsilon_{B3} , \tag{53}$$

$$p_{yB3} = 0 , \tag{54}$$

$$ds = dz_3 , \tag{55}$$

where: σ_{B2} and ε_{B2} are stress and strain in portion B_3 of the integration contour (it should be specified that this portion coincides with the cross-section of the upper crack arm behind the crack tip); ε_{nlspB3} is the strain in the spring, z_3 is the vertical centric axis of the upper crack arm. Therefore,

$$-\frac{h_2}{2} \le z_3 \le \frac{h_2}{2} , \tag{56}$$

where: h_2 is the thickness of the upper crack arm.

We use Eqs.(57), (58), and (59) for analysing the stresses and strains in portion B_3 of the integration contour,

$$\varepsilon_{B3} = \kappa_3 (z_3 - z_{3n}) , \tag{57}$$

$$N_{B3} = \iint_{(A_3)} \sigma_{B3} dA , \tag{58}$$

$$M_{B3} = \iint_{(A_3)} \sigma_{B3} z_3 dA , \tag{59}$$

where:

$$-\frac{h_2}{2} \le z_3 \le \frac{h_2}{2} . \tag{60}$$

Here, κ_3 is curvature, z_{3n} is the neutral axis coordinate, A_3 is the area of the upper crack arm cross-section. Equations (61) and (62) are applied for determining the axial force and the bending moment, N_{B3} and M_{B3},

$$N_{B3} = 0 , \tag{61}$$

$$M_{B3} = \frac{a^2}{2} \int_{-h_2/2}^{h_2/2} f dz_3 . \tag{62}$$

MatLab is used for obtaining κ_3 and z_{3n} from Eqs.(58) and (59). The integration in Eq.(49) is also carried-out by MatLab.

The solution of the J integral is found by substituting Eqs. (21), (35), and (49) in Eq.(20).

The J integral solution is checked-up by deriving the SERR, G. Due to the symmetry, the SERR for the beam in Fig. 1 is found as

$$G = 2G_{oc} , \tag{63}$$

where: G_{oc} is SERR for one crack. The approach reported in /15/ leads to the following result:

$$G_{oc} = \frac{1}{b} \left(\iint_{(A_1)} u^*_{0B1} dA + \iint_{(A_3)} u^*_{0B3} dA - \iint_{(A_2)} u^*_{0B2} dA \right), \tag{64}$$

where: $u_0{}^*_{B1}$, $u_0{}^*_{B2}$, and $u_0{}^*_{B3}$ are reduced specific complementary strain energies in the lower crack arm behind the crack tip, the beam ahead of the crack tip, and the upper crack arm behind the crack tip. Equations (65), (66) and (67) are applied for obtaining the reduced specific complementary strain energies,

$$u^*_{0B1} = \sigma\varepsilon_{nlsp} - \int \sigma d\varepsilon_{nlsp} , \tag{65}$$

$$u^*_{0B2} = \sigma_{B2}\varepsilon_{nlspB2} - \int \sigma_{B2} d\varepsilon_{nlspB2} , \tag{66}$$

$$u^*_{0B3} = \sigma_{B3}\varepsilon_{nlspB3} - \int \sigma_{B3} d\varepsilon_{nlspB3} . \tag{67}$$

MatLab is used for integration in Eq.(64). The SERR found by Eq.(64) matches the solution of the J integral (this fact is a check-up of the solution).

PARAMETRIC ANALYSIS

The parametric analysis presented here aims to evaluate how the lengthwise fracture is influenced by the energy dissipation, beam acceleration, and the distributions of beam mass and the properties of the viscoelastic model across the thickness of the continuously inhomogeneous beam member.

For this purpose, the solution of the J integral in the beam under inertia loads is applied. It is assumed that l 0.800 m, b = 0.020 m, h = 0.028 m, h_1 = 0.015 m, h_2 = 0.015 m, a = 200 m, δ_1 = 0.5, δ_2 = 0.6, and δ_3 = 0.7.

The influence of the distribution of the parameter D across beam thickness on the lengthwise fracture is evaluated first. For this purpose, the change of the J integral caused by variation of D_{llw}/D_{lup} ratio is analysed. The change is presented by graphs reported in Fig. 3.

The continuous reduction of the non-dimensional J integral with growth of D_{llw}/D_{lup} ratio that can be observed in Fig. 3 is induced by increase of beam stiffness. The influence of the energy dissipation is evaluated too. This is done by obtaining the J integral solution assuming that there is no energy dissipation (the corresponding graph is reported in Fig. 3). In order to derive the J integral solution for the case

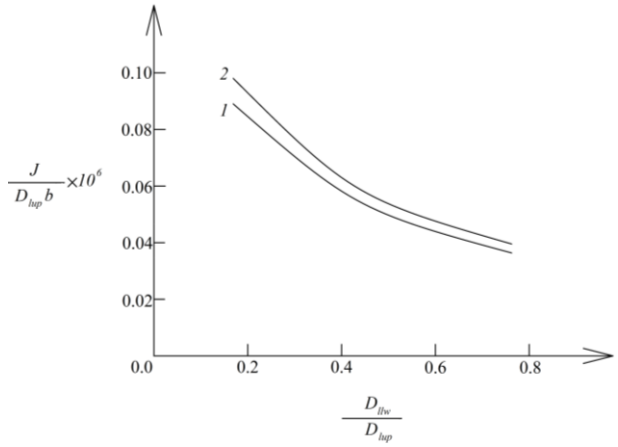

Figure 3. Non-dimensional J integral reported as a function of D_{llw}/D_{lup} ratio (curve 1 - taking into account the energy dissipation, and curve 2 - without taking into account energy dissipation).

when energy dissipation is not taken into account, we determine the specific strain energies that are involved in the expressions of the integral J by integrating the stresses in both spring and dashpot of the viscoelastic model. The graphs in Fig. 3 indicate that energy dissipation leads to the reduction of the J integral.

The influence of mass distribution across the beam thickness on the lengthwise fracture in the moving beam is also evaluated. In this relation, the change of the non-dimensional J integral is presented as a function of m_{llw}/m_{lup} ratio in Fig. 4. The rapid growth of the J integral with increase of the m_{llw}/m_{lup} ratio that can be seen in Fig. 4 is explained by increase of intensities of the distributed inertia load and the deadweight of the beam member. The influence of acceleration on lengthwise fracture is also evaluated. For this purpose, first, the change of J integral due to growth of the n_2/n_1 ratio is analysed. The non-dimensional J integral at three n_2/n_1 ratios is reported in Fig. 4. The growth of the n_2/n_1 ratio induces increase of the J integral (Fig. 4).

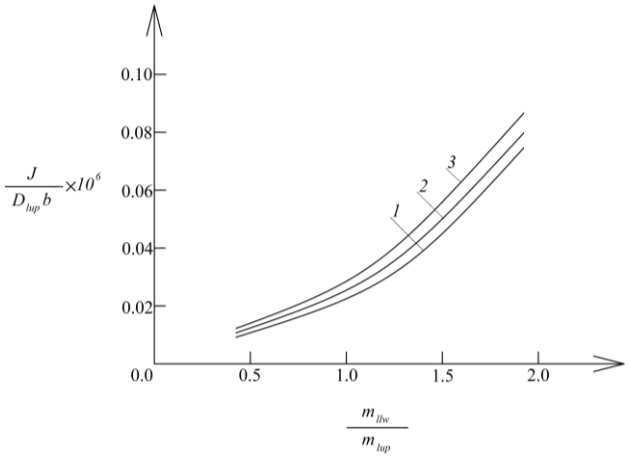

Figure 4. Non-dimensional J integral reported as a function of m_{llw}/m_{lup} ratio (curve 1 - at $n_2/n_1 = 0.5$, curve 2 - at $n_2/n_1 = 1.0$, and curve 3 - at $n_2/n_1 = 1.5$).

It is analysed also how lengthwise fracture is influenced by the continuous change of parameter η across the beam thickness. This influence is illustrated by graphs presenting the non-dimensional J integral as a function of η_{llw}/η_{lup} ratio in Fig. 5. The reduction of J integral with growth of η_{llw}/η_{lup} ratio is due to stiffening of the beam. The influence of *s/r* ratio on the J integral is also illustrated in Fig. 5. The growth of the J integral with increase of *s/r* ratio that can be observed in Fig. 5 is attributed to growth of the intensity of the inertia load acting on the moving beam.

The analysis developed in the current paper can be applied in structural design of nonlinear viscoelastic beams which move with varying acceleration. In particular, the analysis allows us to take into account the influence of the energy dissipation when determining the sizes of the beam member by applying the principles of fracture mechanics. For instance, determination of beam thickness requires the J integral to be obtained at various *h/b* ratios (the corresponding graph is reported in Fig. 6). The beam thickness marked by h_{ed} is found by the condition for equality of the integral J and fracture toughness J_c, as illustrated in Fig. 6. Beam thickness is determined also for the case when energy dissipation is not taken into account (this beam thickness is marked by h_{nd} as shown in Fig. 6). It can be seen in Fig. 6 that taking into account energy dissipation allows us to realize some economy of material (without compromising the safety) since beam thickness is reduced compared to that obtained when energy dissipation in not considered in the structural design (the explanation of this finding consists in the fact that energy dissipation leads to reduction of the amount of energy spent for crack propagation).

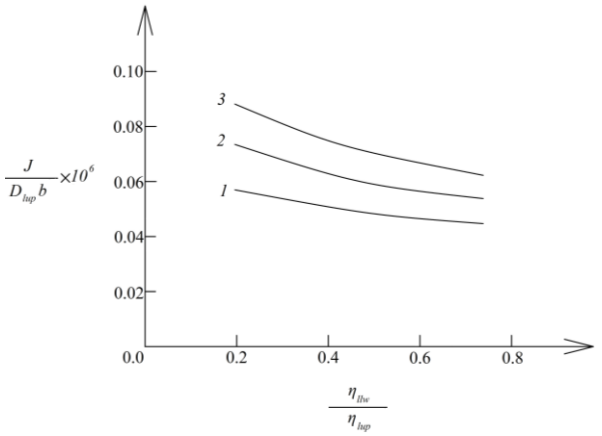

Figure 5. The non-dimensional J integral reported as a function of η_{llw}/η_{lup} ratio (curve 1 - at $r/s = 0.5$, curve 2 - at $r/s = 1.0$, and curve 3 - at $r/s = 1.5$).

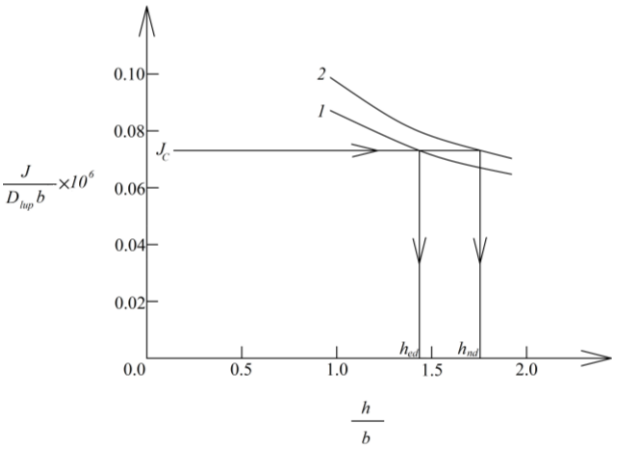

Figure 6. Non-dimensional J integral reported as a function of *h/b* ratio (curve 1 - with taking into account energy dissipation, and curve 2 - without taking into account the energy dissipation).

CONCLUSIONS

The analysis reported in the current paper allows us to evaluate the effect of energy dissipation on the lengthwise fracture in continuously inhomogeneous nonlinear viscoelastic beams moving at a varying acceleration. It is found that taking into account energy dissipation leads to reduction of the J integral. Analysis can be applied in structural design of moving beams by using the principles of fracture mechanics. It is shown that considering the energy dissipation in the structural design allows us to economise material without compromising the safety of moving engineering structures. The effect of various parameters of the theoretical model on lengthwise fracture at taking into account the energy dissipation in the beam is evaluated. It is found that

the J integral reduces when D_{llw}/D_{lup} and η_{llw}/η_{lup} ratios grow. The growth of m_{llw}/m_{lup} ratio causes a rapid increase of J integral value. Increase of the J integral is detected also when n_2/n_1 and s/r ratios grow.

ACKNOWLEDGMENTS

The first author (V.I.R.) would like to thank DAAD for the financial support of his research stay at the Department of Technical Mechanics, Institute of Mechanics, Otto-von-Guericke-University, Magdeburg, Germany.

REFERENCES

1. Suresh, S., Mortensen, A., Fundamentals of Functionally Graded Materials, IOM Communications Ltd., London, 1998.
2. Gasik, M.M. (2010), *Functionally graded materials: bulk processing techniques,* Int. J Mater. Prod. Technol. 39(1-2): 20-29. doi: 10.1504/IJMPT.2010.034257
3. Hedia, H.S., Aldousari, S.M., Abdellatif, A.K., Fouda, N. (2014), *New design of cemented stem using functionally graded materials (FGM)*, Biomed. Mater. Eng. 24(3):1575-1588. doi: 10.3233/bme-140962
4. Udupa, G., Shrikantha Rao, S., Gangadharan, K.V. (2014), *Functionally graded composite materials: an overview*, Procedia Materials Science, 5: 1291-1299. doi: 10.1016/j.mspro.2014.07.442
5. Saiyathibrahim, A., Subramaniyan, R., Dhanapal, P. (2016), *Centrifugally cast functionally graded materials - a review*, In: Int. Conf. on Systems, Science, Control, Communications, Engineering and Technology 2016 (ICSSCCET 2016), Vol.02, pp. 68-73.
6. Mahamood, R.M., Akinlabi, E.T., Functionally Graded Materials, Springer Cham, 2017. doi: 10.1007/978-3-319-53756-6
7. Rizov, V.I. (2018), *Delamination in multi-layered functionally graded beams - an analytical study by using the Ramberg-Osgood equation*, Struct. Integr. Life, 18(1): 70-76.
8. Reichardt, A., Shapiro, A.A., Otis, R., et al. (2021), *Advances in additive manufacturing of metal-based functionally graded materials*, Int. Mater. Rev. 66(1): 1-29. doi: 10.1080/09506608.2019.1709354
9. Li, Y., Feng, Z., Hao, L., et al. (2020), *A review on functionally graded materials and structures via additive manufacturing: from multi-scale design to versatile functional properties*, Adv. Mater. Technol. 5(6): 1900981. doi: 10.1002/admt.201900981
10. Erdogan, F. (1995), *Fracture mechanics of functionally graded materials*, Comp. Eng. 5(7): 753-770. doi: 10.1016/0961-9526(95)00029-M
11. Dowling, N.E., Mechanical Behavior of Materials: Engineering Methods for Deformation, Fracture and Fatigue, 4th Ed., Pearson, 2013. ISBN 0131395068, 9780131395060
12. Rizov, V.I. (2018), *Delamination in nonlinear elastic multi-layered beams of triple graded materials*, Struct. Integr. Life, 18(3): 163-170.
13. Lukash, P.A., Fundamentals of Non-Linear Structural Mechanics, Stroizdat, 1998.
14. Broek, D., Elementary Engineering Fracture Mechanics, Springer Dordrecht, 1986. ISBN 978-90-247-2656-1
15. Rizov, V.I. (2017), *An analytical solution to the stain energy release rate of a crack in functionally graded nonlinear elastic beams*, Eur. J Mech. A/Solids, 65: 301-312. doi: 10.1016/j.euromechsol.2017.04.005